Chemical Engineering Science, Vol. 49, No. 3, pp. 285–301, 1994.
Printed in Great Britain.

0009–2509/94 $6.00 + 0.00

STATE ESTIMATION BASED MODEL PREDICTIVE CONTROL APPLIED TO SHELL CONTROL PROBLEM: A CASE STUDY

ZHENG H. YU, WEI LI and JAY H. LEE†
Department of Chemical Engineering, Auburn University, Auburn, AL 36849, U.S.A.

and

MANFRED MORARI
Chemical Engineering 210-41, California Institute of Technology, U.S.A.

(*First received* 16 *December* 1992; *accepted in revised form* 15 *July* 1993)

Abstract—In this paper, we demonstrate how a practical control problem with multiple control/optimization objectives and various operating constraints is formulated in the theoretical framework of state estimation based model predictive control (SEMPC) proposed by Lee *et al.* We use the shell control problem (SCP) of a heavy oil fractionator as case study. The shell control problem embodies most of the critical elements of challenging industrial process control problems (e.g. unmeasured disturbances, model uncertainty, input/output constraints, optimization objective conflicting with control requirements, failure-prone sensors, secondary measurements, nonsquare system, etc.) and therefore serves as a good test problem for investigation of potential benefits and pitfalls of the new technique. We demonstrate in the case study that, while the theory for the new model predictive control (MPC) technique is rigorously laid out, it is nontrivial for practicing engineers to formulate various practical objectives correctly within the theoretical framework to realize all the potential performance improvements of SEMPC over conventional MPC. By formulating and analyzing a series of different SEMPC controller designs for SCP, this paper highlights some of the possible difficulties that engineers may encounter in applying SEMPC to practical control problems and shows how these difficulties are overcome most efficiently.

1. INTRODUCTION

Model predictive control has emerged as a powerful paradigm for dynamic optimization and control for process industry. Industrial experience with MPC during the past decade has indicated that it is an intuitive and flexible framework to incorporate various practical control objectives and requirements (e.g. constraint handling, conflicting control and optimization objectives, etc.) systematically into the design and implementation of multivariable controllers. In the past decade, MPC has found a wide range of industrial applications, including fluid catalytic crackers, nonlinear batch reactors, hydrocracker reactors, distillation columns, evaporators, autoclaves and other chemical, petroleum-refining and pulp and paper processing operations (Garcia *et al.*, 1989).

Although the initial versions of MPC (referred to as "conventional MPC" from this point on) have found success in many industrial applications, they all share some drawbacks, preventing even broader and more successful implementation in industry. These drawbacks include the complexity and awkwardness in treating large-scale, multivariable systems due to the large state/parameter dimension, inapplicability to unstable processes including the systems with integrating dynamics, poor regulatory performance in the presence of general unmeasured state disturbances, and a high level of experience and effort required for on-line tuning. Most of these drawbacks stem from the fact that conventional MPC uses nonparsimonious impulse/step response models and that its prediction is based on a heuristically designed open-loop disturbance estimator.

Many refinements and extensions to overcome the above-stated limitations have been proposed during the last few years. Li *et al.* (1989) developed a state-space representation of the impulse response model and coupled conventional MPC with the Kalman filter. Lee *et al.* (1992a, b) proposed a state estimation based MPC (SEMPC) technique based on a differenced form of the state-space model (to ensure integral action) and the Kalman filter designed for general stochastic state disturbances. Lee and Yu (1994) developed practical on/off-line tuning rules for the SEMPC controller using the frequency-domain robust control theory (Morari and Zafiriou, 1989). While these developments provide the practicing engineers with more powerful MPC tools that can potentially lead to broader applications and enhanced performance, they also have increased the theoretical complexity of the technique. For example, the use of Kalman filter which, if correctly designed, broadens the applicability of MPC and enhances its performance, can also cause the performance of SEMPC to become inferior to conventional MPC if the practical aspects of the problem are not correctly formulated in the design. Unfortunately, correct mathematical formulation of all the objectives and characteristics of a practical problem is a nontrivial task for most engineers.

†Author to whom correspondence should be addressed.

The key objective of this paper is to provide practicing control engineers with better understandings of the new SEMPC technique so that they can apply it correctly to solve more challenging industrial problems. Some important but nonobvious issues in applying the SEMPC technique include: designing a Kalman filter to estimate the effect of load disturbances on the output without offsets despite model uncertainty; formulating a trade-off objective function that includes control and economic objectives simultaneously; using secondary measurements for faster responses and failure tolerance; efficient tuning of the controller to achieve a desired balance between closed-loop speed and robustness, etc. This paper highlights these issues and provides insights and efficient methods to overcome the above-stated difficulties, by using a well-known benchmark process control problem called "shell control problem (SCP)" as case study. The SCP requires design of a robust control system for a heavy oil fractionator to meet several control and economic objectives despite model uncertainty, constraints and failure-prone measurements. It is an excellent problem for evaluating the effectiveness of a new control technique and providing engineers with required insights and understanding for successful practical application, since it embodies most of the critical elements of typical process control problems. While most of the previous papers on the SCP (Prett *et al.*, 1990) addressed only subsets of the performance and/or optimization objectives, we attempt to present a "complete" solution to the problem.

In order to increase the tutorial value of the paper, we present our complete solution via a sequence of designs, starting with the most simplistic approach of traditional QDMC (a special case of SEMPC) and gradually addressing more issues and aspects of the problem to improve the performance as we progress in the sequence. This way, the effect of certain design modifications on the resulting performance is made transparent to readers. Each of the designs we include to arrive at our final solution is conceivably a design that engineers without adequate understanding of the technique may propose as their final solution.

This paper is organized as follows: In Section 2, we review the theoretical aspects of the SEMPC technique adding some practical insights and interpretations to the theoretical results. In Section 3, the shell control problem is briefly discussed. In Section 4, we present a sequence of five SEMPC designs and simulation results, arriving at our complete solution step by step. Each design and simulation is followed by analysis in which the causes for the observed subpar performance are identified. The simulation results of the final design show that the SEMPC controller, when designed correctly, satisfies all the required objectives and constraints over the given model uncertainty region.

2. STATE-SPACE MPC CONTROL METHODOLOGY

In this section, we review the SEMPC technique presented by Lee *et al.* (1992a, b). While the theoretical aspects of the technique are rigorously laid out in the original papers, we attempt to present them by adding physical insights and interpretations needed for practical application. However, our treatment here will be brief and qualitative. In addition, we will limit our discussion to open-loop stable processes for the sake of simplicity. Readers are referred to the original papers for details and extension to unstable processes.

2.1. *Model*

The following linear state-space model is used in SEMPC:

$$x(k) = Ax(k-1) + B_u u(k-1) + B_d d(k-1) \quad (1)$$

$$y(k) = Cx(k) \quad (2)$$

$$\hat{y}_m(k) = H_m y(k) + v(k). \quad (3)$$

The assumption of open-loop stable dynamics implies that A has all its eigenvalues lying strictly inside the unit disk. H_m is a matrix derived from identity by deleting the rows corresponding to the elements of y whose measurements are not available. d represents the load disturbance and v the measurement noise. In order to apply the optimal state estimation technique, these external signals must be described as white noise of certain covariances. In chemical processes, most load disturbances are "persistent" in nature and therefore are better described as the integrated white noise (Morari and Stephanopoulos, 1980). While such disturbances can be generated by filtering the white noise through integrators, it proves to be more convenient to use the following differenced form where the state equation is expressed in terms of the differenced inputs, Δu and Δd:

$$X(k) = \Phi X(k-1) + \Gamma_u \Delta u(k-1) + \Gamma_d \Delta d(k-1) \quad (4)$$

$$\hat{y}_m(k) = \Theta X(k) + v(k) \quad (5)$$

$$X(k) = \begin{bmatrix} \Delta x(k) \\ y(k) \end{bmatrix}, \quad \Phi = \begin{bmatrix} A & 0 \\ CA & I \end{bmatrix}$$

$$\Theta = [0_{n_{ym}, n_x} \quad H_m]$$

$$\Gamma_u = \begin{bmatrix} B_u \\ CB_u \end{bmatrix} \quad \Gamma_d = \begin{bmatrix} B_d \\ CB_d \end{bmatrix}.$$

Δd and v are modeled as white noise of covariances R_d and R_v. Note that the white noise assumption of Δd makes d an integrated white noise vector that describes the persistent characteristics of typical load disturbances well. Δd can also be made colored noise by further augmenting the model with dynamics obtained from the spectral factorization of the spectrum of Δd [see Lee *et al.* (1992a) for detail].

2.2. *State estimation using Kalman filter*

To develop prediction of the future behavior of the output for MPC, the current state vector $X(k)$ needs to be estimated from the measurements. For continuous processes, the steady-state Kalman filter minimizing a scalar measure of the estimation error

covariance matrix is a logical choice. Let us use the notation of $X(k|l)$ to denote the estimate of $X(k)$ based on measurements up to time l. Given the measurement $\hat{y}(k)$ and previous estimate $X(k-1|k-1)$, the steady-state Kalman filter constructs the new estimate $X(k|k)$ in the following way (Åström and Wittenmark, 1984):

$$X(k|k-1) = \Phi X(k-1|k-1) + \Gamma_u \Delta u(k-1) \quad (6)$$

$$X(k|k) = X(k|k-1) + K_f[\hat{y}_m(k) - \Theta X(k|k-1)]. \quad (7)$$

K_f is the steady-state Kalman filter gain matrix obtained via the following formula:

$$K_f = \Sigma\Theta^T(R_v + \Theta\Sigma\Theta^T)^{-1} \quad (8)$$

where Σ is the solution to the following algebraic Riccati equation (ARE):

$$\Sigma = \Phi\Sigma\Phi^T + \Gamma_d R_d \Gamma_d^T - \Phi\Sigma\Theta^T(R_v + \Theta\Sigma\Theta^T)^{-1}\Theta\Sigma\Phi^T. \quad (9)$$

The solution Σ is called a "stabilizing solution" if the corresponding Kalman filter gain [obtained through eq. (8)] is such that all the eigenvalues of $\Phi - K_f\Theta\Phi$ (referred to as the "observer poles") lie strictly inside the unit disk. This condition ensures asymptotic convergence of the state estimates to the true states despite arbitrary initial error. There are two important requirements in order that the above ARE has a unique, stabilizing solution (Goodwin and Sin, 1984):

(1) (Θ, Φ) is a detectable pair.
(2) $(\Phi, \Gamma_d R_d^{1/2})$ has no unstabilizable mode on the unit circle.

Although it is straightforward to check the above requirements, their implications must be understood for correct application of the Kalman filter. The first condition is needed for the existence and uniqueness of a "strong" solution to ARE (9). A strong solution places all the observer poles (i.e. eigenvalues of $\Phi - K_f\Theta\Phi$) inside or on the unit circle. This implies that, while the estimates from the observer are guaranteed not to diverge *exponentially* from the true states (for an arbitrary initial estimation error), it is not guaranteed that they converge to the true states asymptotically. The second condition ensures that the strong solution is actually "stabilizing", implying the asymptotic convergence of the estimates to the true states.

Comments on condition 1. It is important to understand the implications of the condition since many practical problems of interest may violate it (although in a specific way). In model of eqs (4) and (5), (Θ, Φ) is detectable if and only if H_m has full column rank. The requirement implies that the system is always undetectable when there are unmeasured outputs. However, the physical interpretation of Σ (i.e. the steady-state error covariance of the optimal estimates), suggests that a strong solution, although nonunique, may still exist in some cases since the undetectable dynamics are simple integrators in this case. The condition for the existence of a strong solution is that the integrators corresponding to the unmeasured outputs are not excited by the external disturbance Δd that is unobservable from $\hat{y}_m$. Mathematically, the condition is

$$\text{Ker}\{H_{um}C(I-A)^{-1}B_d R_d^{1/2}\} \supset \text{Ker}\{H_m C(I-A)^{-1}B_d R_d^{1/2}\} \quad (10)$$

where Ker denotes the null-space and H_{um} is a matrix that extracts the unmeasured outputs from y. Note that $\text{Ker}\{H_{um}C(I-A)^{-1}B_d R_d^{1/2}\}$ represents the part of the disturbance space that is not exciting the unmeasured output and $\text{Ker}\{H_m C(I-A)^{-1}B_d R_d^{1/2}\}$ is the part that is not observable from $\hat{y}_m$. The condition says that the latter should belong to the former.

A strong solution to ARE (9) can be found by iterating the Riccati difference equation corresponding to the ARE (Goodwin and Sin, 1984). It can be shown that the optimal filter gain K_f is unique although strong solution is not unique (Lee *et al.*, 1992a). In addition, K_f places all the observer poles strictly inside the unit disk except for those integrators on the unmeasured outputs. However, this implies that offsets result in the estimates of the unmeasured outputs. This is an inherent limitation that can only be removed by including additional measurements.

Comments on condition 2. The second condition implies that, unless all the unstable modes on the unit circle are excited by Δd, the resulting strong solution may not (actually necessarily not) be stabilizing, implying offsets in the estimates. Note that for system (4) and (5), the condition is violated if and only if the matrix $C(I-A)^{-1}B_d R_d^{1/2}$ does not have full row rank. This means that, when the total number of load disturbances specified in the design is less than the total number of outputs, the resulting steady-state Kalman filter will leave offsets. This property should be intuitive since the steady-state Kalman filter is designed to reject only the disturbances specified in the model and none else. In practice, offsets can be caused in two ways: the initialization errors in the states (that are unaccounted for since we are using the steady state Kalman filter), and state errors that are unaccounted for by Δd in the model, such as those due to unmodeled disturbances and model errors. On the contrary to condition 1, condition 2 is not an inherent limitation, however, since one can always specify additional disturbances (accounting for these unmodeled errors) to satisfy the condition. This will be the approach we take later in the case study to ensure that the resulting steady-state Kalman filter is stabilizing.

2.3. *Prediction*

We can extend the idea used in Kalman filtering to develop multistep prediction of future output. Noting

that, on the basis of the measurements up to time k, $E\{\Delta d(k+i)\} = 0, \forall i \geqslant 0$ and $E\{X(k) - X(k|k)\} = 0$, the following optimal prediction equation can be derived:

$$\mathscr{Y}(k+1|k) = \mathscr{S}^x \Delta x(k|k) + \mathscr{S}^p y(k|k) + \mathscr{S}^u \Delta \mathscr{U}(k) \tag{11}$$

where

$$\mathscr{Y}(k+1|k) = \begin{bmatrix} y(k+1|k) \\ y(k+2|k) \\ \vdots \\ y(k+p|k) \end{bmatrix}$$

$$\Delta \mathscr{U}(k) = \begin{bmatrix} \Delta u(k) \\ \Delta u(k+1) \\ \vdots \\ \Delta u(k+m-1) \end{bmatrix}$$

$$\mathscr{S}^p = \begin{bmatrix} I_{n_y} \\ I_{n_y} \\ \vdots \\ I_{n_y} \end{bmatrix}, \quad \mathscr{S}^x = \begin{bmatrix} CA \\ CA^2 + CA \\ \vdots \\ \sum_{j=1}^{p} CA^j \end{bmatrix}$$

$$\mathscr{S}^u = \begin{bmatrix} CB_u & 0 & \cdots & 0 \\ CAB_u + CB_u & CB_u & \cdots & 0 \\ \vdots & \vdots & \ddots & \vdots \\ \sum_{j=1}^{p} CA^{j-1}B_u & \sum_{j=1}^{p-1} CA^{j-1}B_u & \cdots & \sum_{j=1}^{p-m+1} CA^{j-1}B_u \end{bmatrix}. \tag{12}$$

We have included in the equation the flexibility of suppressing the last $p - m$ input moves *a priori* (i.e. $\Delta u(k+m) = \cdots = \Delta u(k+p-1) = 0$) for reduced computation and more flexible tuning of MPC.

2.4. *Control move calculation*

Given the prediction equation (11) and the future reference vector $\mathscr{R}(k+1|k) = [r^T(k+1|k), r^T(k+2|k), \cdots, r^T(k+p|k)]^T$ at time k, $\Delta \mathscr{U}(k)$ containing the present and future manipulated input moves is calculated by minimizing a chosen measure of the weighted predicted tracking error $[\mathscr{Y}(k+1|k) - \mathscr{R}(k+1|k)]$ and weighted $\Delta \mathscr{U}(k)$ over the prediction horizon. The quadratic norm is the most popular choice of the measure and the optimization to be solved in this case is

$$\min_{\Delta \mathscr{U}(k)} \{ \| \Lambda_y [\mathscr{Y}(k+1|k) - \mathscr{R}(k+1|k)] \|_2^2 + \| \Lambda_u \Delta \mathscr{U}(k) \|_2^2 \}. \tag{13}$$

The weighting matrices Λ_y and Λ_u are often chosen in the form of

$$\text{diag}\left(\overbrace{\tilde{\Lambda}_y, \cdots, \tilde{\Lambda}_y}^{p}\right) \quad \text{and} \quad \text{diag}\left(\overbrace{\tilde{\Lambda}_u, \cdots, \tilde{\Lambda}_u}^{m}\right)$$

where $\tilde{\Lambda}_y$ and $\tilde{\Lambda}_u$ are matrices of dimensions n_y and n_u, respectively, adjusted to achieve the desired trade-off between the closed-loop speed and robustness for different variables. Other on-line adjustable parameters include the prediction and control horizons p and m.

In the absence of constraints, the optimal solution for (13) can be written explicitly in the following form:

$$\Delta \mathscr{U}(k) = K_{MPC}[\mathscr{R}(k+1|k) - \mathscr{S}^x \Delta x(k|k) - \mathscr{S}^p y(k|k)] \tag{14}$$

where

$$K_{MPC} = ((\mathscr{S}^u)^T \Lambda_y^T \Lambda_y \mathscr{S}^u + \Lambda_u^T \Lambda_u)^{-1} (\mathscr{S}^u)^T \Lambda_y^T \Lambda_y. \tag{15}$$

In the presence of constraints, optimization (13) is solved via quadratic programming (Ricker, 1985). The control moves are implemented in a receding horizon fashion, i.e. only the current control move $\Delta u(k)$ is implemented and the same optimization is repeated at the next time step with the updated prediction equation, etc.

2.5. *Failure tolerant cascaded Kalman filter with on-line tuning parameters*

In many process control problems including SCP, the measurements of key variables are subject to failures. While it is possible to store the optimal Kalman filter gains for all the potential measurement failure scenarios, such an approach to ensure tolerance to measurement failures often requires unnecessarily much design efforts. Lee *et al.* (1992b) showed that, for superior failure tolerance, a simple suboptimal Kalman filter equipped with intuitive on-line tuning parameters can be used instead. They also concluded that the suboptimal estimator suffers negligible performance loss over the optimal estimator in the case that the unreliable output measurements accompany dynamics of large time constants or delays. Our presentation of the technique here will be succinct and qualitative; readers are referred to Lee *et al.* (1992a) for more rigorous derivations and proofs.

The proposed suboptimal filter is in a cascaded form consisting of the "main" and "auxiliary" estimators designed in a sequential manner (see Fig. 1). Assume that the outputs are ordered in such a way that the first n_{y+} elements of y represent the reliable measurements and the rest those unavailable or prone to frequent failures. Hence,

$$y(k) = \begin{bmatrix} y^+(k) \\ y^-(k) \end{bmatrix}$$

where $y^+(k)$ and $y^-(k)$ represent the output vectors of reliable and failure-prone/unavailable measurements, respectively. First, the main estimator is designed using only the reliable measurements. Hence, the

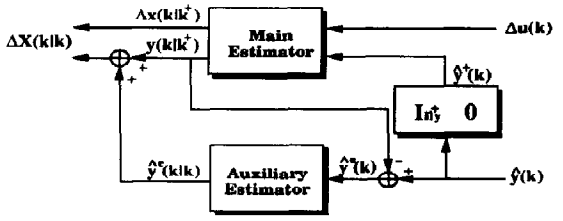

Fig. 1. Cascaded Kalman filter with on-line tuning parameters and superior failure tolerance property.

measurement equation (3) used in the full Kalman filter design is replaced by

$$\hat{y}^+ = H^+ y(k) + v^+(k). \tag{16}$$

The superscript $\{\cdot\}^+$ represents the part of the vector or the matrix corresponding to the outputs that are reliably measured (e.g. $H^+ = [I_{n_{y^+}} \; 0]$). We denote the steady-state Kalman filter gain for eqs (4)/(16) as K_f^+. The estimates for $\Delta x(k)$ and $y(k)$ from the Kalman filter are also denoted as $\Delta x(k|k^+)$ and $y(k|k^+)$, respectively.

It is noteworthy that, because $\hat{y}^+$ does not include full $y(k)$, the system is undetectable. However, as mentioned earlier, a strong solution to ARE (9) exists as long as $\text{Ker}\{H^-C(I-A)^{-1}B_dR_d^{1/2}\} \supset \text{Ker}\{H^+C(I-A)^{-1}B_dR_d^{1/2}\}$, where H^- and H^+ are the matrices that extract y^- and y^+ from y, respectively. The latter condition is *always* satisfied if $H^+C(I-A)^{-1}B_dR_d^{1/2}$ has full row rank (i.e. there are more reliable measurements than linearly independent disturbances). Certainly, it makes sense to include as many reliable measurements as the number of load disturbances for failure-tolerant control [if not, see Lee *et al.* (1992a) on how to modify the matrix R_d in an optimal manner to satisfy the condition]. K_f^+ calculated from a strong solution places all the observer poles strictly inside the unit disk except for those integrators on y^-.

Due to the unstabilized integrators on the output $y^-(k)$ the main estimator gives biased estimates for $y^-(k)$. This bias can be corrected by cascading the main estimator with an auxiliary estimator that uses all the measurements including the unreliable ones. Let us denote the errors in the estimates $y(k|k^+)$ as $y^e(k)$, i.e. $y^e(k) = y(k) - y(k|k^+)$. These errors cannot be modeled exactly because they may arise from several unquantifiable sources (e.g. initialization errors, unmodeled disturbances, model errors, etc.). Since we are mainly interested in removing the bias, y^e can be modeled simply as independent, integrated, white noise. In other words, we may use the following model for the auxiliary estimator design:

$$y^e(k) = y^e(k-1) + w(k-1) \tag{17}$$

$$\hat{y}^e(k) = y^e(k) + v(k) = \hat{y}(k) - y(k|k^+). \tag{18}$$

$w(k)$ and $v(k)$ are white noise with *diagonal* covariances. The steady-state Kalman filter gain for the above model is explicitly parameterized as follows:

$$K_f^e = \begin{bmatrix} f & & \\ & \ddots & \\ & & f_{n_y} \end{bmatrix} \tag{19}$$

where f_i is a parameter taking the value between 0 and 1 and is determined according to the signal-to-noise ratio of the respective output (i.e. ratio between the ith diagonal element of the covariance matrix of $w(k)$ and that of $v(k)$). Since such a covariance matrix is not readily available *a priori* in most cases, f_i may be adjusted on-line instead.

If the ith measurement fails (or is unavailable at the first place), f_i can be simply set to zero (which corresponds to zero signal-to-noise ratio). Because a diagonal noise model is assumed, a failure of one measurement should not affect the estimates of the other variables. In addition, the main estimator ensures that certain integrity in the estimate of the "lost" output is maintained, a very desirable failure tolerance feature. The overall estimator can be implemented either in a cascaded form as shown in Fig. 1 or as an equivalent single observer in the form of eqs (6) and (7) with K_f replaced by K_{cas}:

$$K_{cas} = \left[\left(I - \begin{bmatrix} 0_{n_x,n_y} \\ K_f^e \end{bmatrix}[0_{n_y,n_x} \quad I_{n_y}]\right) \times [K_f^+ \quad 0_{n_x,n_y}]\right] + \begin{bmatrix} 0_{n_x,n_y} \\ K_f^e \end{bmatrix} \tag{20}$$

where, $0_{n_x,n_y}$ is a zero matrix with n_X rows and n_y columns.

While the integrated white-noise model (17) for $y^e(k)$ suffices in most cases, if the system contains integrating dynamics or dynamics of large time constants, a more elaborate model (such as the integrated white noise filtered through first-order dynamics of an appropriate time constant) may be necessary for more efficient removal of bias. Although not shown here, similar parameterizations of the optimal filter gains for such models are also available and can be found in Lee *et al.* (1992b). However, this creates additional states (corresponding to the first-order dynamics for y^e) that need to be included in the output prediction equation (11).

3. PROBLEM DESCRIPTION OF SHELL CONTROL PROBLEM

3.1. *General description*

The SCP put forward by the research group at Shell Development asks for design of a control system for a heavy oil fractionator (shown in Fig. 2) with five inputs and seven outputs such that given performance, optimization, constraints and failure tolerance requirements are met over a specified model uncertainty region. The main control objective is to keep the top and side draw compositions y_1 and y_2 (controlled variables) at their setpoints in the face of varying loads in the upper and intermediate reflux duties d_1 and d_2 (unmeasured disturbances). The problem

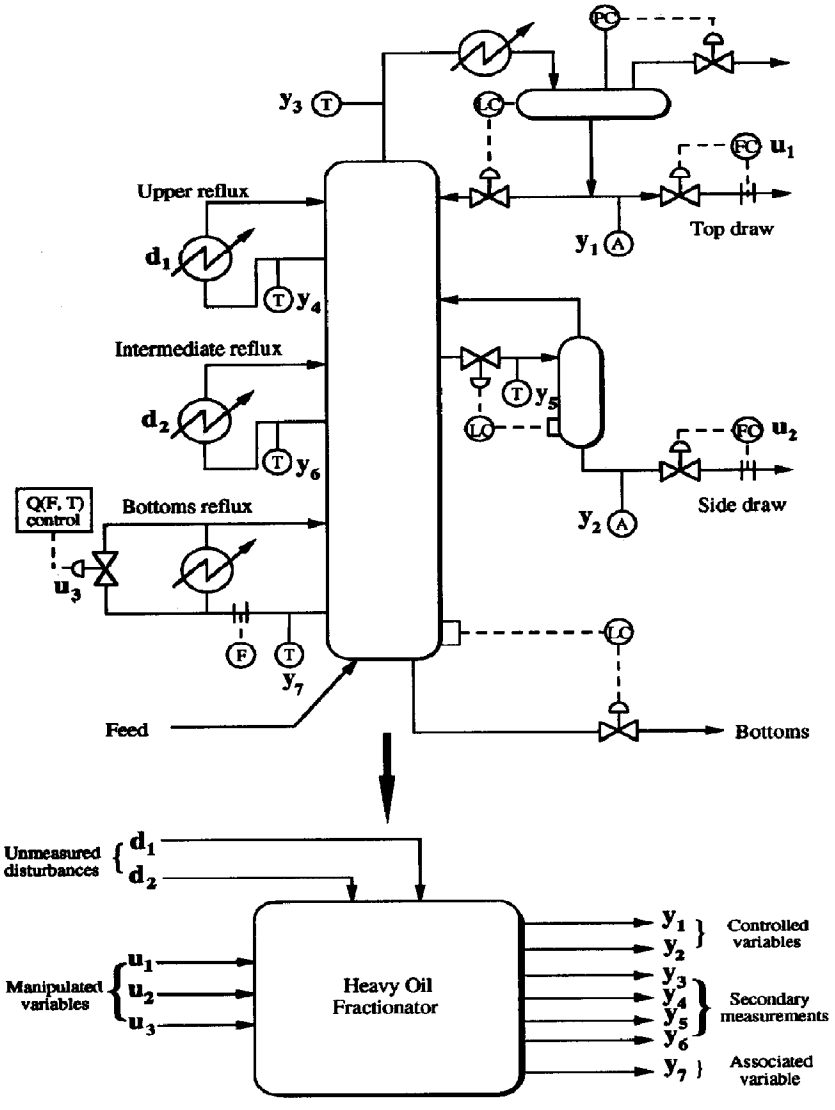

Fig. 2. Diagram of a heavy oil fractionator and associated control problem.

also features the bottom reflux draw temperature (y_7) as an associated variable that must be kept above certain lower limit. Other four outputs (y_3, y_4, y_5, y_6) are secondary temperature measurements which may be used for inferential control. Three manipulated variables, the top draw (u_1), side draw (u_2) and bottom reflux duty (u_3), are used to achieve this objective. In addition to the control objective, the problem includes an economic objective: in order to maximize the heat recovery, u_3 must be mininized without compromising the composition control objectives. Each input/output dynamics is modeled via a first-order transfer function with a delay. The complete model and its associated uncertainty can be found in Prett and Morari (1987).

3.2. *Objectives, constraints and prototype cases*

The exact control objectives and constraints for the SCP are outlined as follows:

Control objectives:

(1) Maintain y_1 and y_2 at specification without offsets (0.0 ± 0.005 at steady state);
(2) Maximize steam make in the steam generators (i.e. maximize heat recovery) in the bottom circulating reflux, that is u_3 should be minimized;
(3) Reject the unmeasured disturbances d_1 and d_2 due to changes in heat duty requirements from other columns. The anticipated range of variations for the unmeasured disturbances are:

$-0.5 \leqslant d_1 \leqslant 0.5$; $-0.5 \leqslant d_2 \leqslant 0.5$. Reject disturbances even when one or both end point analyzers fail.

(4) Achieve close-loop speed response for y_1 and y_2 between 0.8 and 1.25 times that of the open-loop speed of response.

Control constraints

(1) $-0.5 \leqslant u_1 \leqslant 0.5$, $-0.5 \leqslant u_2 \leqslant 0.5$, $-0.5 \leqslant u_3 \leqslant 0.5$;
(2) $|\Delta u_1| \leqslant 0.05$, $|\Delta u_2| \leqslant 0.05$, $|\Delta u_3| \leqslant 0.05$;
(3) sampling time $\geqslant 1$ min;
(4) $-0.5 \leqslant y_1 \leqslant 0.5$, $y_7 \geqslant -0.5$.

The designed controller should satisfy all the above control objectives without violating the given constraints over the region of model parameter space representing the model uncertainty.

Prototype test cases:

Load disturbances d_1 and d_2 vary between -0.5 and 0.5. The uncertain gain parameters ε_i, $i = 1, 2, \ldots, 5$ given in the model vary between $+1$ and -1. Since it is impossible to test all possible combinations of load disturbances and uncertainty parameters, SCP comes with five prototype cases which supposedly represent the most relevant model uncertainty/disturbance combinations to render a fair evaluation of a designed controller's performance. All inputs and outputs are assumed to be zero initially. Magnitudes for the upper and intermediate reflux duty step changes and particular uncertainty parameter combinations for the tested prototype cases are indicated below:

Case 1: No model uncertainty. $d_1 = 0.5$, $d_2 = 0.5$.

Case 2: $\varepsilon_1 = \varepsilon_2 = \varepsilon_3 = -1$, $\varepsilon_4 = \varepsilon_5 = 1$; $d_1 = -0.5$, $d_2 = -0.5$.

Case 3: $\varepsilon_1 = \varepsilon_2 = \varepsilon_3 = \varepsilon_4 = 1$, $\varepsilon = -1$; $d_1 = -0.5$, $d_2 = -0.5$.

Case 4: $\varepsilon_1 = \varepsilon_2 = \varepsilon_3 = \varepsilon_4 = \varepsilon_5 = 1$; $d_1 = 0.5$, $d_2 = -0.5$.

Case 5: $\varepsilon_1 = -1$, $\varepsilon_2 = 1$, $\varepsilon_3 = \varepsilon_4 = \varepsilon_5 = 0$; $d_1 = -0.5$, $d_2 = -0.5$.

4. SIMULATION AND RESULTS

In this section, we present our SEMPC designs for the SCP outlined in the previous section. In order to enhance the tutorial value of this paper, we present a series of five designs, starting with the simplest SEMPC design (that amounts to traditional QDMC) and gradually adding more objectives and features of the problem to arrive at our final solution. By doing so, it is hoped that the effect of each modification made in the design will become transparent to readers. Each design and simulation results are followed by analysis to help readers gain insights to solve the particular difficulties that they may encounter in practice.

4.1. *Design A—QDMC design*

Controller design. In our first design, instead of the given disturbance model, we use a simple disturbance model of integrated white noise added directly to each output (see Fig. 3). All the output measurements $(y_1, y_2, y_3, y_4, y_5, y_6, y_7)$ are included in the design. Hence, our model used for the design is

$$\begin{bmatrix} \Delta x(k) \\ y(k) \end{bmatrix} = \begin{bmatrix} A & 0 \\ CA & I \end{bmatrix} \begin{bmatrix} \Delta x(k-1) \\ y(k-1) \end{bmatrix} + \begin{bmatrix} B_u \\ CB_u \end{bmatrix} \Delta u(k-1) + \begin{bmatrix} 0 \\ I \end{bmatrix} w(k-1) \quad (21)$$

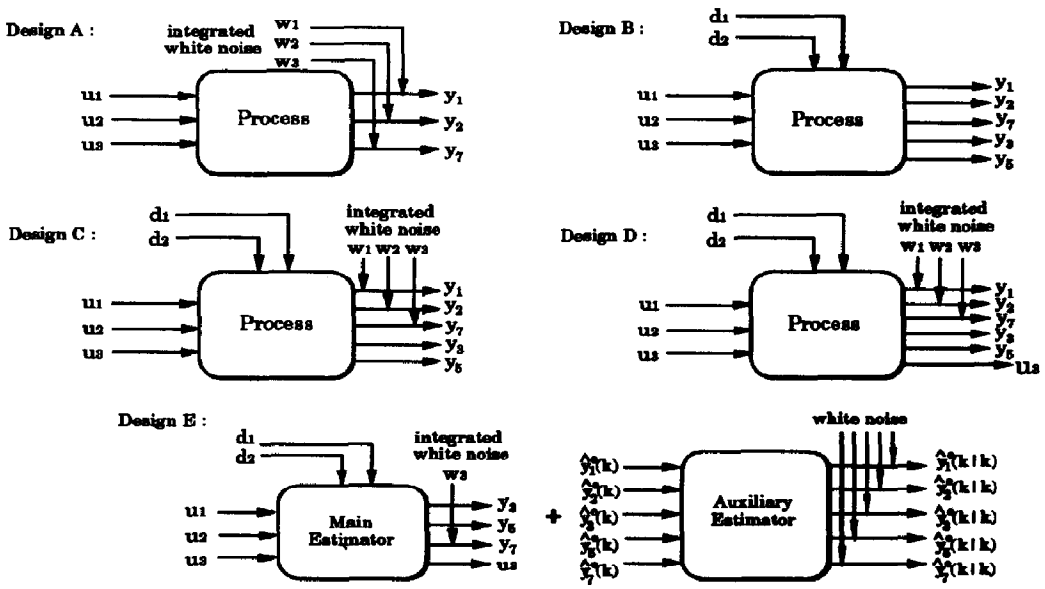

Fig. 3. Schematic diagrams of models for SEMPC designs.

$$\hat{y}(k) = y(k) + v(k) \tag{22}$$

where $w(k)$ is white noise of a diagonal covariance matrix. Note that it is the same disturbance model used in the auxiliary estimator design for the cascaded Kalman filter. When measurement noise is assumed to be negligible, the SEMPC controller based on the above model is equivalent to the traditional QDMC controller. In addition to the objective function, all the relevant constraints were incorporated into the algorithm.

The following parameterizations for the design/tuning parameters were used:

$$p = 40, \quad m = 10, \quad \tilde{\Lambda}_y = \text{diag}\{1\ \ 1\ \ 0\ \ 0\ \ 0\ \ 0\ \ 0\}$$

$$\tilde{\Lambda}_u = \alpha \times \text{diag}\{1\ \ \beta\ \ \gamma\}, \quad R_w = I_7, \quad R_v = 0.$$

The sampling time we used is 2 min. The prediction/control horizons were chosen as large as possible within the computational limit. It was found that using horizons larger than 40 and 10 respectively did not improve the performance. Equal importance was given to both end point compositions and the zero weight was assigned to the associated variable y_7, since this variable only has to be kept above its lower limit. In addition, the zero weights were assigned to the secondary variables y_3–y_6 since no control requirements were specified for these variables. Infinite signal-to-noise ratios were assumed to make the resulting controller equivalent to the QDMC controller. α is a parameter that adjust the relative weighting between the output and input penalty terms. β is a parameter to weigh the inputs u_1, u_2 differently in the input penalty term. It was expected that the flexibility of assigning different weights on these inputs would improve the performance because of the different gains associated with them. The γ parameter was used for penalizing the bottom reflux duty differently as well since it had an optimization requirement. These three parameters (α, β and γ) were adjusted for best simulation results. The best values obtained after a heuristic three-dimensional search are: $\alpha = 1.5$, $\beta = 0.1$ and $\gamma = 1$. While a more elaborate, global search for the optimal choices of p, m, $\tilde{\Lambda}_y$ and $\tilde{\Lambda}_u$ is possible, we rejected this idea since such a tuning approach would be highly impractical. Whenever the constraints were declared "infeasible" by the QP algorithm, we softened them by removing the constraints for the particular time step.

Simulation results and analysis. Simulation results of the designed controller for all the prototype test cases are shown in Fig. 4. The results show that the controller rejects disturbances with no offset for all the test cases despite model uncertainty. This is expected since the independent integral white-noise disturbance model assumed in the design forces integral action on each output.

Note, however, the constraints for the controlled variable (y_1) and associated variable (y_7) are violated during transients in cases 2, 3 and 5. In addition, the settling time for compositions is about 300 min. which is within the design requirements but somewhat sluggish. Because the disturbance is assumed to enter each output independently in the QDMC design, the "fast" secondary temperature measurements are not used to infer the endpoint compositions. This makes control action to be taken only after the load disturbances affect the compositions and the significant delays in the process transfer functions cause sluggish settling and constraint violation. We emphasize that the sluggish performance cannot be improved regardless of tuning.

In addition to the sluggish closed-loop response, it should be obvious that, when a composition measurement is lost, the integrity of the estimate for this composition is completely lost since no other measurements can be used to update this output. This fact is clearly demonstrated in the simulation results shown in Fig. 5, where simulation is carried out using the Kalman filter designed without the top composition measurement. We conclude that, unless the full disturbance model is used for state estimation, the secondary measurements play *no role* in SEMPC. Our next design naturally replaces the simple output disturbance model with the full state disturbance model provided by the SCP.

4.2. *Design B—SEMPC design with full state disturbance model*

Controller design. In our second design, in order to achieve better transient performance and constraint handling, we design an SEMPC controller with a state estimator utilizing the full state disturbance model (see Fig. 3). To eliminate the disturbance effect efficiently, the control moves must become active before they affect the compositions. We should be able to use the temperature measurements ($y_3, \ldots, y_7$) without delays to predict the future effect of the disturbances on the compositions and activate the control inputs as early as possible to compensate for the significant process delays.

While it is possible to use all the available temperature measurements, we select and use only two of them (y_3, y_5) in order to reduce the controller complexity. In our case, two measurements turn out to be sufficient for inference of the compositions since there are only two unmeasured load disturbances. The selection of the particular secondary measurements was made via a systematic method (Lee and Morari, 1991), but will not be discussed in this paper. The following tuning parameters are used for the SEMPC controller:

$$p = 40, \quad m = 10, \quad \tilde{\Lambda}_y = \text{diag}\{1\ \ 1\ \ 0\ \ 0\ \ 0\}$$

$$\tilde{\Lambda}_u = 1.5 \times \text{diag}\{1\ \ 0.1\ \ 1\}, \quad R_d = I_2, \quad R_v = 0.$$

We choose the same values of the prediction horizon p, control horizon m, weighting matrices $\tilde{\Lambda}_y$ and $\tilde{\Lambda}_u$ as in the last design. The noise covariance was set to zero such that the closed-loop speed and robustness would be determined by the input weight only (as in LQG/LTR).

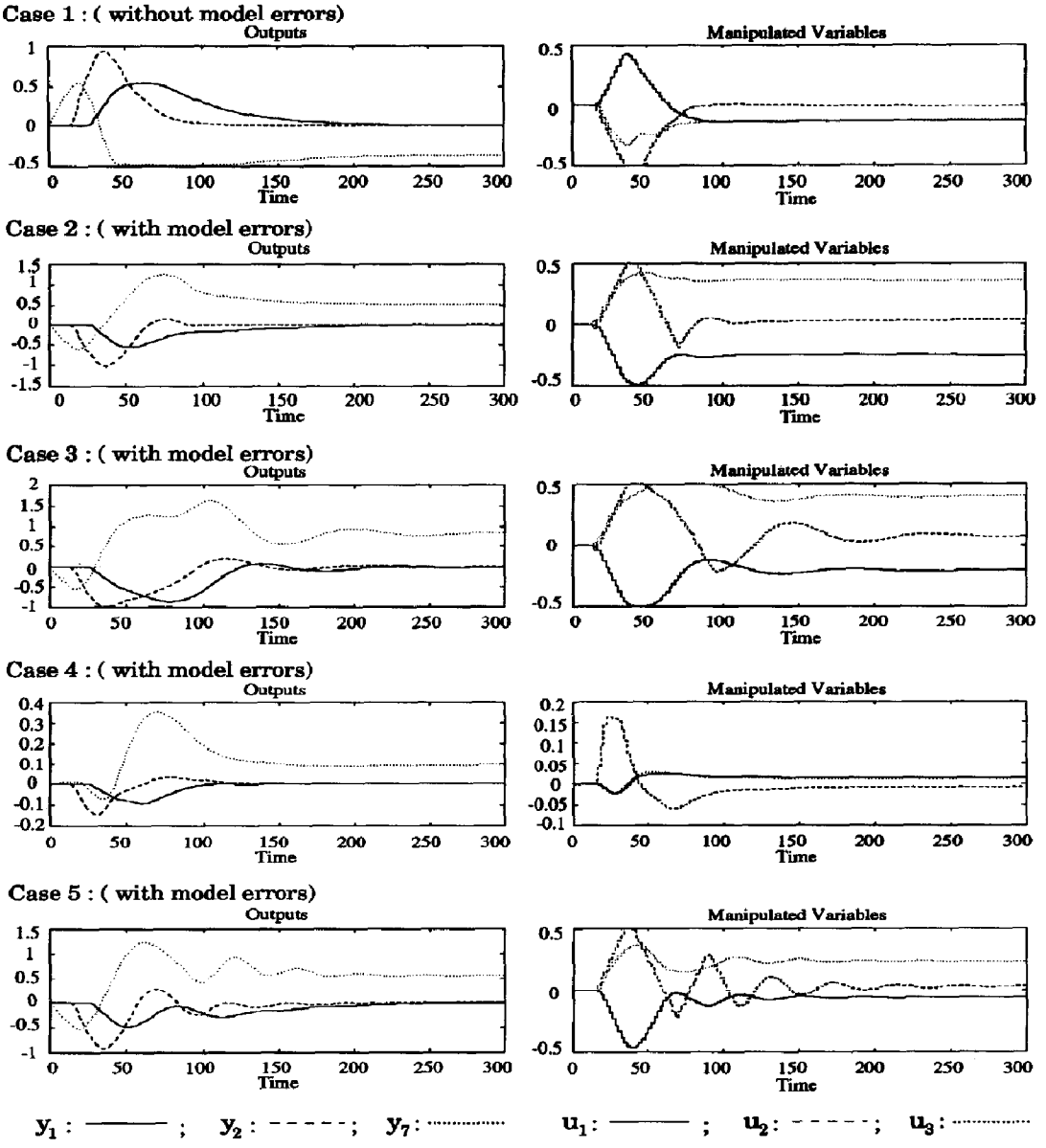

Fig. 4. Design A: closed-loop responses QDMC controller.

Simulation results and analysis. The simulation results in Fig. 6 show that the SEMPC controller generates much faster control moves, resulting in more efficient disturbance rejection. The settling time is less than 150 min for all the prototype test cases. Unlike in design A, control moves become active immediately after the disturbances occur because the "fast" temperature measurements can be now used to predict the future effect of disturbances on the compositions. The outputs (y_1 and y_7) are far from reaching their constraints. In summary, the overall transient performance is much better than that we got from design A.

However, upon closer inspection of the simulation results for cases 2–5, we note that both endpoint compositions show offsets in the presence of model errors. This is counter-intuitive since the composition measurements should enable us to control them without steady-state bias despite model errors if the controller indeed had integral action on these outputs. Indeed, these offsets are not inherent, but a consequence of a naive Kalman filter design. Because we specified only two load disturbances (which was modeled to be integrated white noise) in the Kalman filter design, the resulting controller has integral action on only two linear combinations of the five out-

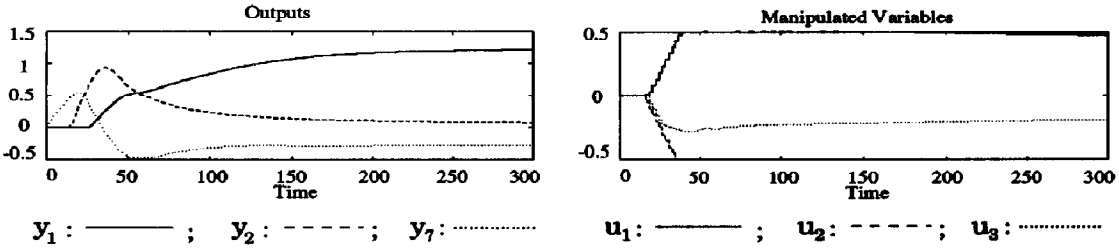

Fig. 5. Design A: closed-loop responses of QDMC controller during y_1 composition measurement failures for prototype case 1.

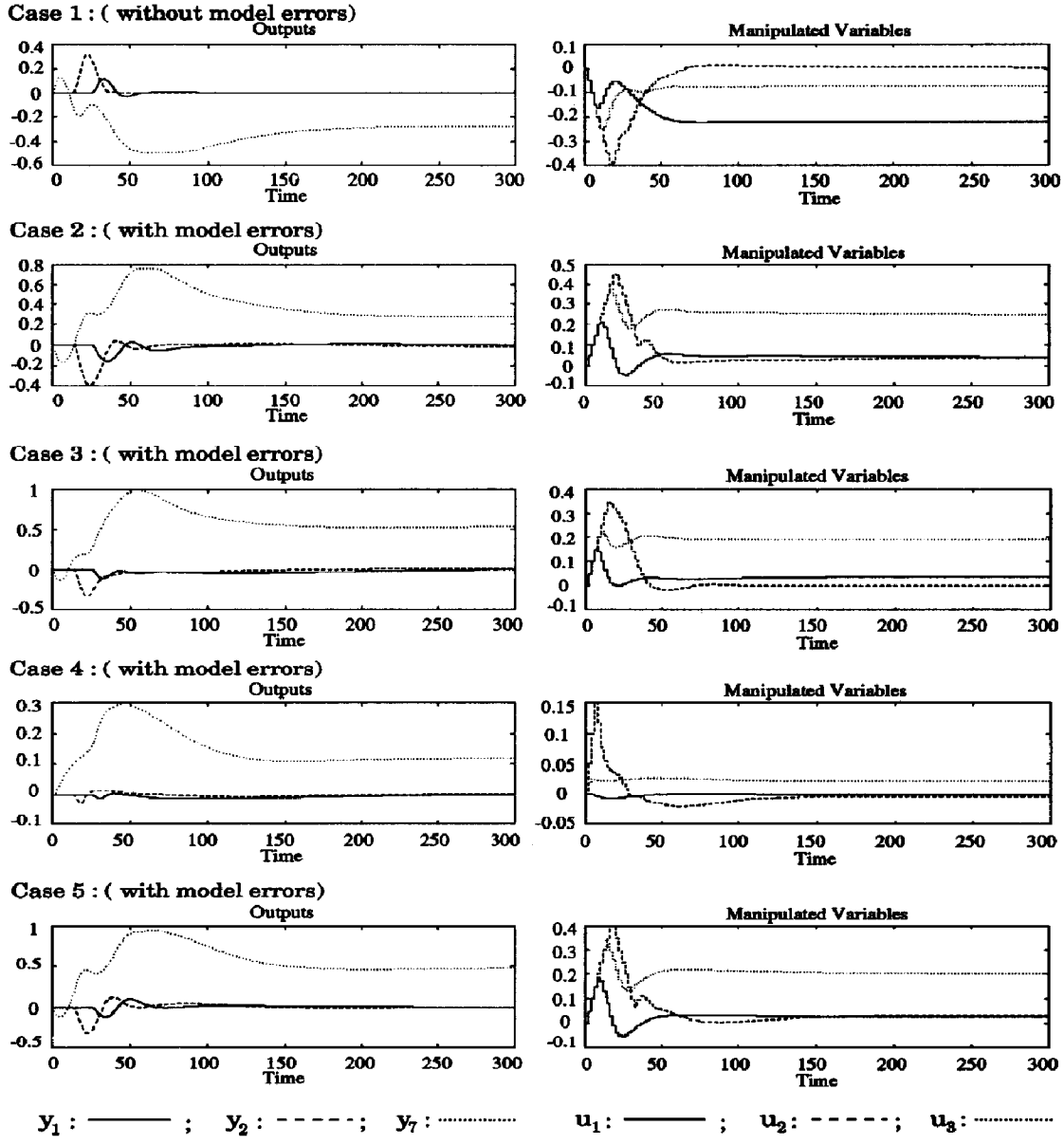

Fig. 6. Design B: closed-loop responses of SEMPC controller with load disturbance model.

puts. Mathematically, we can interpret this as the violation of the second condition for the stabililty of the Kalman filter (addressed in Section 2.2). It is interesting to note that these unstable observer poles manifest themselves as output offsets only when there are model errors. The unstable observer poles are never excited when there are no model errors or unmeasured disturbances not included in the model.

This particular problem of steady-state offsets caused by the unequal number of outputs and disturbances is a very likely one in practice, but not an inherent one. We will show how it can be overcome efficiently in our next design.

4.3. *Design C—SEMPC with combined load/output disturbance models*

Controller design. In the previous design, we observed offsets in the endpoint compositions if the model had errors in it. The offsets cannot be eliminated regardless of how the controller is tuned. We attributed this unexpected phenomena to the fact that the number of load disturbances specified for the Kalman filter design is less than the number of outputs. This will cause the output estimates to be biased in the presence of model errors despite their measurements.

A logical solution to this problem is to modify the disturbance model used for the Kalman filter to ensure unbiased estimates of the compositions. This can be easily done by adding integrated white-noise disturbances to each output as shown in Fig. 3. In this context, we must modify the model that we use for the Kalman filter design as follows:

$$\begin{bmatrix}\Delta x(k)\\ y(k)\end{bmatrix}=\begin{bmatrix}A & 0\\ CA & I\end{bmatrix}\begin{bmatrix}\Delta x(k-1)\\ y(k-1)\end{bmatrix}+\begin{bmatrix}B_u\\ CB_u\end{bmatrix}\Delta u(k-1)+\begin{bmatrix}B_d & 0\\ CB_d & I\end{bmatrix}\begin{bmatrix}\Delta d(k-1)\\ w(k-1)\end{bmatrix} \tag{23}$$

$$\hat{y}(k)=y(k)+v(k). \tag{24}$$

Note that the external state disturbance vector now consists of two parts: the differenced form of the original load disturbances, $\Delta d(k)$, provided by the SCP and the output disturbances, $w(k)$, added by us. Both $\Delta d(k)$ and $w(k)$ are modeled as white noise, but are integrated through the integrators present on the states y. The output disturbances can be interpreted as errors in the output estimates that are caused by the model errors or unmodeled disturbances. The use of such output disturbances are not at all uncommon; the traditional MPC techniques such as DMC and IMC rely exclusively on them to enforce integral action.

The tuning parameters we get for this design strategy are:

$p = 40, \quad m = 10$

$\tilde{\Lambda}_y = \text{diag}\{1\ \ 1\ \ 0\ \ 0\ \ 0\}, \quad \tilde{\Lambda}_u = 1.5 \times \text{diag}\{1\ \ 0.1\ \ 1\}$

$R_d = I_2, \quad R_w = \delta \times \text{diag}\{1\ \ 1\ \ 1\ \ 0\ \ 0\}, \quad R_v = 0.$

We use the same tuning parameters that we used in the last design. The only extra parameter we needed to specify is R_w, which was chosen to have the particular structure shown above to simplify the tuning. Note that the covariances of the output disturbances for y_3 and y_5 were set to zero *a priori*. While it is entirely possible to add disturbances to all five outputs, we added such disturbances only to y_1, y_2 and y_7 in this application. First, the addition of the three disturbances makes the total number of independent disturbances to be equal to the number of outputs. Hence, the condition for the stability of the Kalman filter which was violated in the earlier design, is now satisfied. Second, because we have no control requirements on the secondary temperature outputs y_3 and y_5, the accuracy of their estimates were not of our concern. δ is a tuning parameter that determines the balance between the modeled load disturbance effects and errors due to model errors at the outputs. Note that, as δ goes to zero, we are back to our previous design and the speed for the elimination of the output bias becomes slower. A satisfying value of δ found through trial and error was 0.01.

Simulation and analysis. The simulation results for the SEMPC controller with the modified Kalman filter are presented in Fig. 7. In all of the five test cases, the controller controls both endpoint compositions without steady-state offsets, while maintaining the same excellent transient performance that we saw for design B. The new design combines the advantages of both the traditional QDMC and the state estimation based MPC using the state disturbance model.

One of the issues for the SCP that we have not addressed thus far in our design is the optimization of the bottom reflux duty. In the next design, we will formulate the optimization requirement for the bottom reflux duty as a secondary objective and incorporate it into the SEMPC objective function.

4.4. *Design D—SEMPC design including the optimization objective*

Controller design. The SCP states that, in order to maximize the heat recovery, u_3 must be minimized *without* compromising the composition control requirements. Although it appears that sufficient degrees-of-freedom exist for *independent* composition control and optimization, the third manipulated variable u_3 is also needed for the composition control because of the constraints on y_7 as well as those on u_1 and u_2. Hence, the optimization clearly interacts with the control of the two compositions: any extensive adjustment in u_3 causes composition deviations and can cause offsets for the composition control system. The minimum reachable value for the bottom reflux duty without violating the control requirements for the endpoint compositions will vary from one time to another, depending on the nature of the current disturbances and plant parameters. Hence, u_3 would

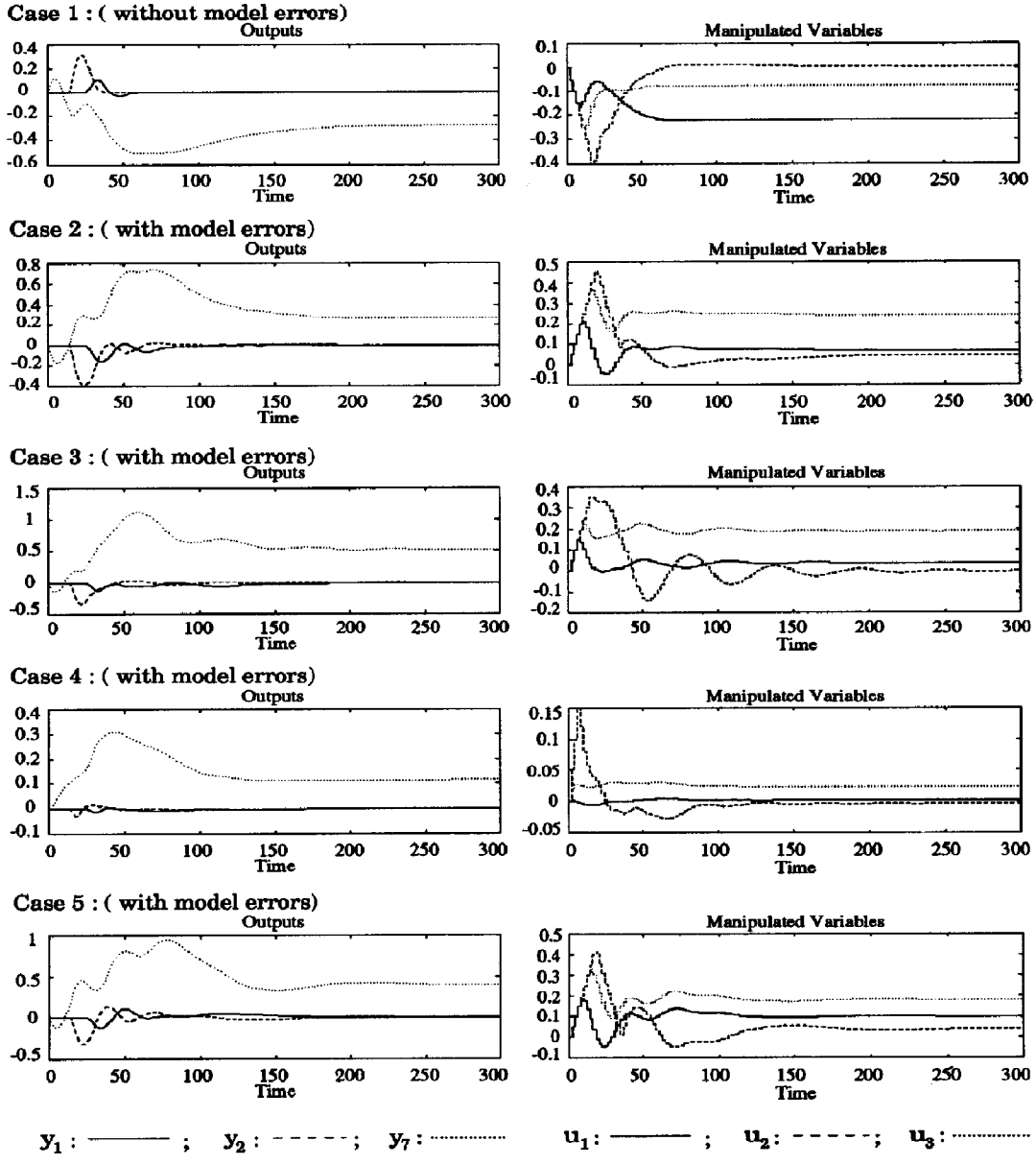

Fig. 7. Design C: closed-loop responses of SEMPC controller with load/output disturbance model.

have to be determined iteratively and continuously adapted on-line during operation. The model-based dynamic optimization of u_3 is impractical since the disturbances are not measured and the model is imperfect.

This dilemma can be solved efficiently by creating a trade-off objective function that includes u_3 as a controlled variable as shown in Fig. 3. With the extra output, the output weight is modified to have the following structure:

$$\Lambda_y = \text{diag}\{1 \quad 1 \quad 0 \quad 0 \quad 0 \quad \xi\}. \tag{25}$$

ξ is the parameter that determines the trade-off between the control requirements and the optimization requirement. Since the control requirements should not be compromised in our case, we should set ξ to be very small. ξ was set equal to 0.01. All the other design parameters were left at the values used in the previous design.

This simple approach allows the setpoint for u_3 to be kept constant, therefore eliminating the need for complex on-line adaptation. The setpoint can be set to any value as long as it is chosen below the minimum achievable value under *all* operating conditions. We determined this value to be -0.22 and set the setpoint at this value for our simulation.

Simulation results, analysis and improvement. Simulation results are shown in Fig. 8. We observe that, counter to our expectation, the results obtained are not too different from those for design C. The reason for this is that, because ξ is chosen so small relative to the input weight $\tilde{\Lambda}_u$, the speed of u_3 reaching its optimal value is extremely slow. The only way we can speed it up is to increase ξ or decrease $\tilde{\Lambda}_u$. The former is unacceptable since this would lead to a sacrifice in the composition control. The latter is a feasible approach, but one would lose the robustness since the resulting controller would be too tightly tuned. However, this particular fact can be compensated for by using a nontrivial measurement noise covariance.

Based on this idea, we have detuned the SEMPC controller with the following choice of the parameters:

$$p = 40, \quad m = 10$$

$$\tilde{\Lambda}_y = \text{diag}\{1 \;\; 1 \;\; 0 \;\; 0 \;\; 0 \;\; 0.01\}$$

$$\tilde{\Lambda}_u = 0.1 \times \text{diag}\{1 \;\; 0.1 \;\; 1\}$$

$$R_d = I_2, \quad R_w = \text{diag}\{0.5 \;\; 0.5 \;\; 100\}$$

$$R_v = \text{diag}\{\lambda \;\; \lambda \;\; \mu \;\; \mu \;\; \mu\}.$$

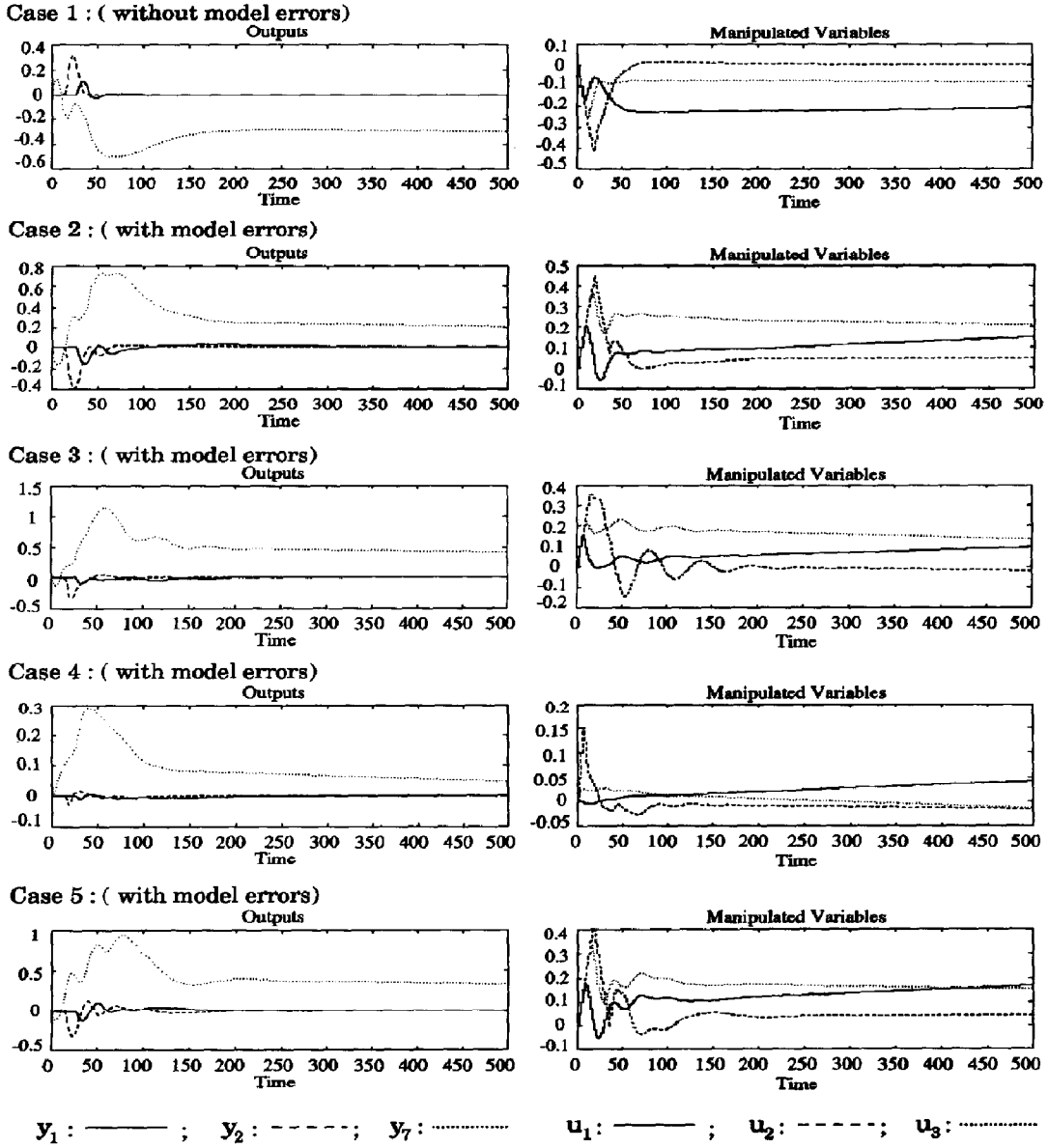

Fig. 8. Design D(a): closed-loop responses of SEMPC controller with optimization objective included—tuned with input weight.

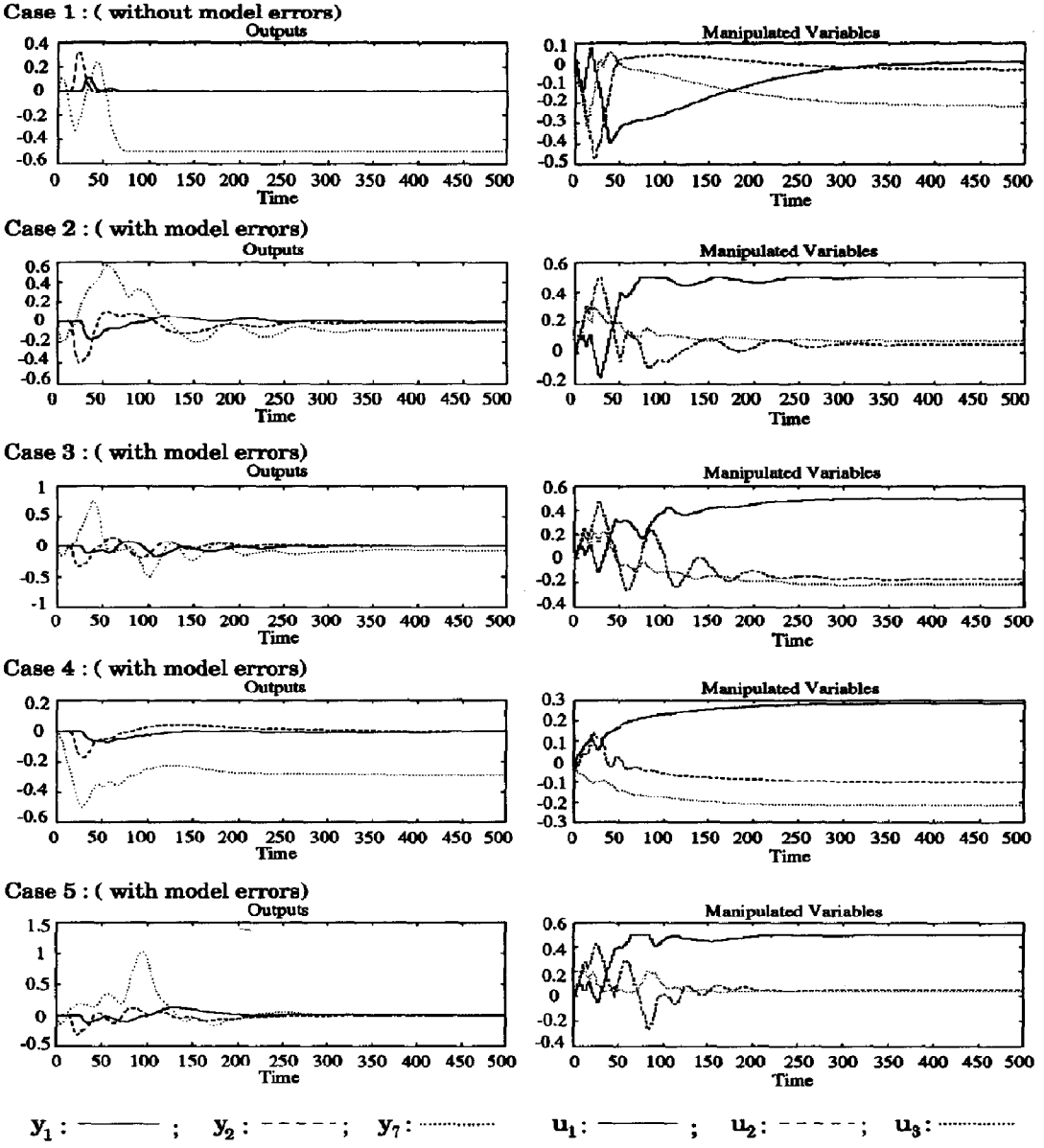

Fig. 9. Design D(b): closed-loop responses of SEMPC controller with optimization objective included—tuned with noise covariances.

Note that we decreased the input weight $\tilde{\Lambda}_u$ significantly to speed up the optimization, and increased the noise covariance R_v to make up for the reduced robustness margin. In choosing the noise covariance, a balance had to be struck between the generality and required tuning effort. Two parameters were optimized as shown above, λ and μ corresponding to the noise variances for the composition and temperature measurements, respectively. The heuristic search showed that the best values are $\lambda = 1$ and $\mu = 3$. Simulation results for the new design are presented in Fig. 9. The u_3 value is lower than the previous design for every prototype test cases. Moreover, u_3 reaches the minimum values much faster than the previous design. All the other desirable traits of design C are retained.

We note that the incorporation of the optimization objective in such a simple manner would not have been possible for the QDMC controller since it does not give the user the flexibility of achieving the robustness via tuning parameters of the state estimator.

4.5. *Design E—SEMPC design with cascaded Kalman filter for failure tolerance*

Controller design. The final aspect of the SCP that needs to be addressed now is the control system's

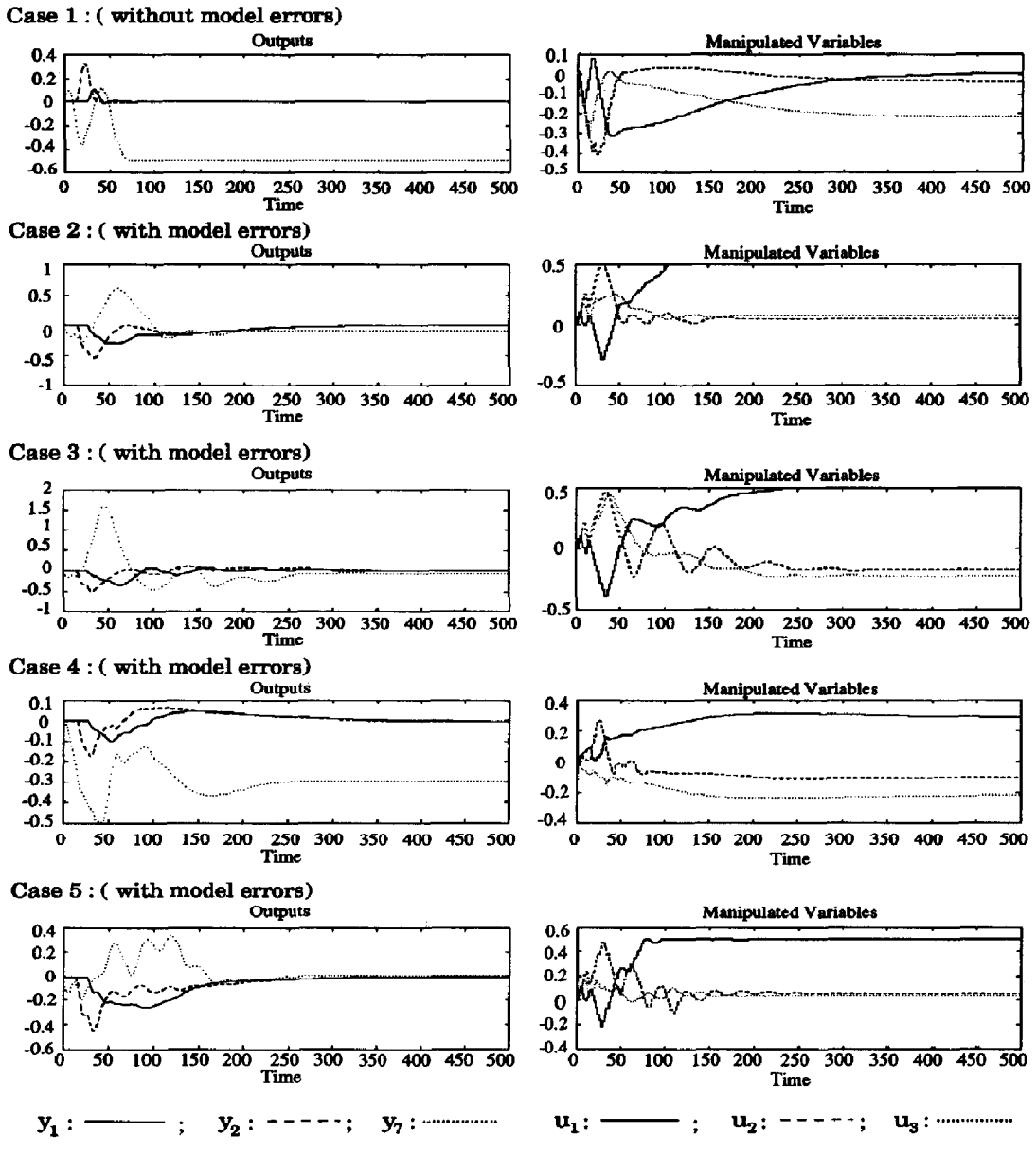

Fig. 10. Design E: closed-loop responses of the SEMPC controller with cascaded Kalman filter.

tolerance to the composition measurement failures. Failure tolerance is often an important practical requirement for control system design since many measurement devices (such as those for composition measurements) are unreliable and require frequent servicing. In the SCP, the failures of the two endpoint analyzers may cause some undesirable changes to the closed-loop performance. It is our objective to modify our controller design so that these undesirable changes are minimized and the integrity of the control system is maintained.

We meet this important requirement by replacing the Kalman filter with the cascaded Kalman filter discussed in Section 2.5. The main estimator was designed with the temperature measurements only. The composition measurements were excluded for the main estimator design in view of their frequent operational failures. Of course, the output disturbances w were excluded from the model for the design (except w_3 which was added to y_7) so that a strong solution for the Riccati equation can be found. All the design parameters for MPC and the state estimators were chosen to be same as in design D. The auxiliary estimator was designed using all the measurements including the composition measurements. The auxiliary estimator gain used for the simulation was

$$K_f^e = \text{diag}\{1 \quad 1 \quad 1 \quad 0.9 \quad 0.9 \quad 1\}. \tag{26}$$

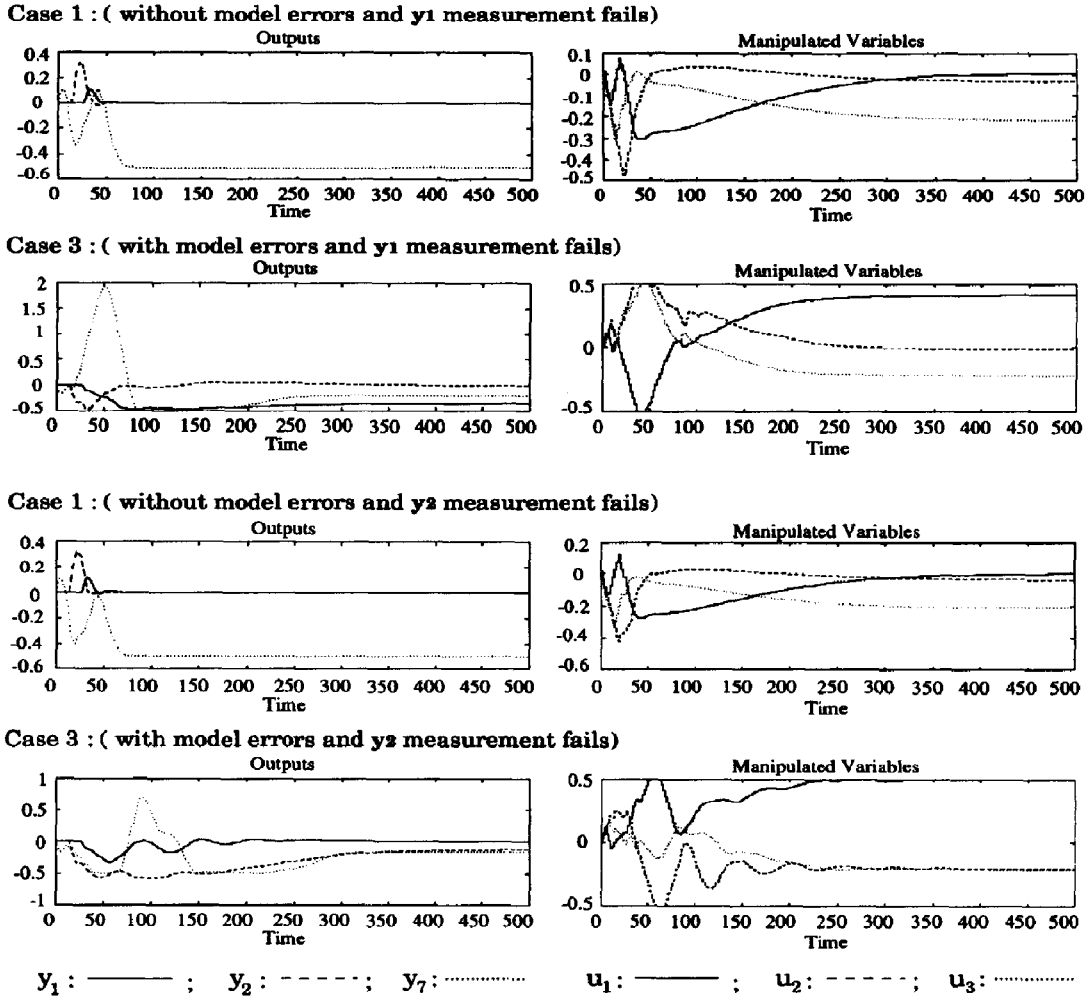

Fig. 11. Design E: closed-loop responses of the SEMPC controller when y_1 or y_2 composition measurements fail.

Simulation results, analysis and improvement. The simulation results for the SEMPC controller with the cascaded Kalman filter are shown in Fig. 10. We observe that the responses obtained are very similar to those for design D. Apparently, due to the large delays associated with the composition measurements, they had contributed little to the transient performance of the controller, even when the optimal Kalman filter was used. Their primary role was not much more than removing the bias in the composition estimates, and, hence, the transient performance of the suboptimal cascaded estimator is equally as good.

Figure 11 shows the closed-loop responses when y_1 or y_2 composition measurements fail. As we observe, the integrity of the closed-loop system is adequately maintained during these failures. It is natural that, in the presence of model errors, offset results for the composition of which cannot be measured.

5. CONCLUSIONS

In this paper, we presented a tutorial of the new SEMPC technique by Lee *et al.* (1992a, b) emphasizing its application aspects. We used a well-known benchmark process control problem developed by Shell Development as case study. The use of secondary measurements allowed by the state estimation based approach significantly improved the closed-loop response speed, disturbance rejection, constraint handling and failure handling over conventional MPC. However, we encountered in the process a number of issues that needed to be correctly formulated within the theoretical framework of SEMPC in order to achieve the desired result. While these issues are nonobvious to most practicing engineers, they have significant impact on the final result. We attempted to highlight these issues and their impact

on the resulting closed-loop performance by presenting a series of designs leading to the final solution.

Acknowledgement—JHL gratefully acknowledges the financial support from National Science Foundation (CTS #9209808) and the Pulp and Paper Research and Education Center at Auburn University.

NOTATION

$A, B_u,$ B_d, C	matrices used in a state-space representation of the system
d	load disturbance
d_1, d_2	load disturbances in the upper and intermediate reflux duties
H_{um}	matrix that extracts the unmeasured outputs
H_m	matrix that extracts the measured outputs
K_f	Kalman filter gain
K_{cas}	cascaded Kalman filter gain
K_f^e	auxiliary Kalman filter gain
m	size of the input move horizon
p	size of the prediction horizon
R_d, R_v, R_w	covariance matrices for the disturbance, measurement noise and output disturbance
u	manipulated input vector
u_1, u_2, u_3	manipulated variables; top draw, side draw and bottom reflux duty
w	output disturbance vector
x	system states
X	augmented system states
y	system outputs
$\hat{y}$	system measurements
y_1, y_2	controlled variables; top and side draw compositions
$y_3, y_4,$ y_5, y_6	secondary temperature measurements
y_7	associated variable; bottom reflux draw temperature

Greek letters

α	tuning parameter to balance the output and input penalty terms
β	tuning parameter to weight different inputs
γ	tuning parameter to penalize the bottom reflux duty
δ	tuning parameter to balance the output disturbance and load disturbances
ξ	tuning parameter to balance the composition control and optimization
λ, μ	tuning parameters for noise variance of the composition and temperature measurements
v	measurement noise
$\Phi, \Gamma_u,$ Γ_d, Θ	matrices used in an augmented state-space representation of the system
Δ	differenced value
Σ	solution to the algebraic Riccati equation
$\bar{\Lambda}_y, \bar{\Lambda}_u$	output and input weighting matrices

Superscripts

$+$	reliable measurement
$-$	unavailable measurement
e	error estimates

Subscripts

d	load disturbance
m	reliable measurement
u	system input
um	unavailable measurement
w	added disturbance
y	system output
v	measurement noise

REFERENCES

Åström, K. J. and Wittenmark, B., 1984, *Computer Controlled Systems: Theory and Design.* Prentice-Hall, Englewood Cliffs, NJ.

Garcia, C. E., Prett, D. M. and Morari, M., 1989, Model predictive control: theory and practice—a survey. *Automatica* **25**, 335–348.

Goodwin, G. C. and Sin, K. S., 1984, *Adaptive Filtering Prediction and Control.* Prentice-Hall, Englewood Cliffs, NJ.

Lee, J. H., Gelormino, M. S. and Morari, M., 1992a, Model predictive control of multi-rate sampled-data systems: a state-space approach. *Int. J. Control* **55**, 153–191.

Lee, J. H. and Morari, M., 1991, Robust measurement selection. *Automatica* **27**, 519–528.

Lee, J. H., Morari, M. and Garcia, C. E., 1992b, State space interpretation of model predictive control. *Automatica* (accepted).

Lee, J. H. and Yu, Z., 1994, Tuning of model predictive controllers for robust performance. *Comput. chem. Engng* **18**, 15–37.

Li, S., Lim, K. Y. and Fisher, D. G., 1989, A state space formulation for model predictive control. *A.I.Ch.E. J.* **35**, 241–249.

Morari, M. and Stephanopoulos, G., 1980, Minimizing unobservability in inferential control schemes. *Int. J. Control* **31**, 367–377.

Morari, M. and Zafiriou, E., 1989, *Robust Process Control.* Prentice-Hall, Englewood Cliffs, NJ.

Prett, D. M., Garcia, C. E. and Ramaker, B. L., 1990, *The Second Shell Process Control Workshop.* Butterworths, Stoneham, MA.

Prett, D. M. and Morari, M., 1987, *Shell Process Control Workshop.* Butterworth, Stoneham, MA.

Ricker, N. L., The use of quadratic programming for constrained internal model control. *Ind. Engng Chem. Process Des. Dev.* **24**, 925–936.